Electronic Supplementary Material (ESI) for ChemComm.

Supplementary information

A Novel Supramolecular Metallogel-Based High-Resolution Anions Sensor Array

Qi Lin,*[a] Tao-Tao Lu,[a‡] Xin Zhu,[a‡] Bin Sun,[a] Qing-Ping Yang,[a] Tai-Bao Wei,[a] You-Ming Zhang*[a,b]

[a]*Key Laboratory of Eco-Environment-Related Polymer Materials, Ministry of Education of China, Key Laboratory of Polymer Materials of Gansu Province, College of Chemistry and Chemical Engineering, Northwest Normal University, Lanzhou, Gansu, 730070, P. R. China.*

[b]*Key Laboratory of Hexi Corridor Resourses Utilization of Gansu, Hexi University, Zhangye, Gansu, 734000, P. R. China.*

Table of Contents

Materials and instruments

Synthesis of gelator G1

Scheme S1. Synthesis of the gelator **G1**.

Table S1 . Gelation Property of Organogelator **G1**

Figure S1. a) Plots of CGCs of **G1** in the different solvents. b) Plots of T_{gel} against the concentrations of organogel **OG** and metalogels **CuG** in DMF.

Figure S2. Photographs of organogel of **G1** in DMF (1% w/v) and organogels of **G1** in the presence of various metal ions (using their perchlorate salts as the sources, **G1**: cation =2 : 1) under (a) room (b) UV light.

Figure S3. Fluorescence spectra of organogel of **G1** in DMF (0.8% w/v) and organogels of **G1** in the presence of various metal ions (using their perchloric salts as the sources) added in 2 : 1 mol ratio with respect to **G1** (λ_{ex} = 380 nm)**.**

Figure S4. Fluorescence responses of the metallogels-based sensor to the presence of 1 equiv. of anions mixture (a water solution containing the mixture of F^-, Cl^-, Br^-, I^-, AcO^-, $H_2PO_4^-$, N_3^-, SCN^-, S^{2-}, ClO_4^- and CN^-). (a_1) **CuG**; (a_2) **CuG** and anions; (b_1) **FeG**; (b_2) **FeG** and anions; (c_1) **CrG** and **HgG**; (c_2) **CrG** and anions, **HgG** and anions; (d_1) **ZnG**; (d_2) **ZnG** and anions.

Figure S5. a) Fluorescence spectra of **FeG** (1.0%, in DMF) with increasing concentration of CN^- (using 1.0 mol L^{-1} NaCN water solution as the CN^- sources), λ_{ex} = 380 nm; b) Fluorescence spectra of **HgG** (1.0%, in DMF) with increasing concentration of SCN^- (using 0.1 mol L^{-1} KSCN water solution as the SCN^- sources), λ_{ex} = 380 nm; c) Fluorescence spectra of **CrG** (1.0%, in DMF) with increasing concentration of S^{2-} (using 0.01 mol L^{-1} Na_2S water solution as the S^{2-} sources), λ_{ex} = 380 nm; d) Fluorescence spectra of **ZnG** (1.0%, in DMF) with increasing concentration of I^- (using 0.1 mol L^{-1} KI water solution as the I^- sources), λ_{ex} = 380 nm.

Figure S6. Time-dependency fluorescence spectra of a) **CuG** film treated with CN^-, 0.01 mol L^{-1} NaCN water solution as the CN^- sources, λ_{ex} = 380 nm; b) **FeG** film treated with CN^-, 0.01 mol L^{-1} NaCN water solution as the CN^- sources, λ_{ex} = 380 nm; c) **HgG** film treated with SCN^-, 0.01 mol L^{-1} KSCN water solution as the SCN^- sources, λ_{ex} = 380 nm; d) **CrG** film treated with S^{2-}, 0.01 mol L^{-1} Na_2S water solution as the S^{2-} sources, λ_{ex} = 380 nm; e) **ZnG** film treated with I^-, 0.01 mol L^{-1} KI water solution as the I^- sources, λ_{ex} = 380 nm

Figure S7. FT-IR spectra of powdered **G1** and xerogel of organogel **OG**.

Figure S8. Powder XRD patterns of xerogel of **OG**, **CuG**, and **CuG** xerogel treated with CN^-.

Figure S9. SEM images of (a) and (b) **OG** xerogel; (c) and (d) **CuG** xerogel and (e) and (f) **CuG** xerogel treated with CN- in situ.

Scheme S2. Chemical structure of the **G1** and the assumed self-assembly and stimuli-responsive mechanism.

Materials and instruments

All reagents and starting materials were obtained from commercial suppliers and used as received unless otherwise noted. All anions were used as sodium or potassium salts while all cations were used as the perchlorate salts, which were purchased from Alfa Aesar and used as received. Fresh double distilled water was used throughout the experiment. Nuclear magnetic resonance (NMR) spectra were recorded on Varian Mercury 400 and Varian Inova 600 instruments. Mass spectra were recorded on a Bruker Esquire 6000 MS instrument. The X-ray diffraction analysis (XRD) was performed in a transmission mode with a Rigaku RINT2000 diffractometer equipped with graphite monochromated CuKa radiation (λ = 1.54073 Å). The morphologies and sizes of the xerogels were characterized using field emission scanning electron microscopy (FE-SEM, JSM-6701F) at an accelerating voltage of 8 kV. The infrared spectra were performed on a Digilab FTS-3000 Fourier transform-infrared spectrophotometer. Melting points were measured on an X-4 digital melting-point apparatus (uncorrected). Fluorescence spectra were recorded on a Shimadzu RF-5301PC spectrofluorophotometer.

Synthesis of gelator G1

Synthesis of gelator **G1**.Compounds 3,4,5-tris(hexadecyloxy)benzo-hydrazide were synthesized according to literatures methods.[1] **G1** was synthesized as follow: quinoline-2-carbaldehyde (1 mmol), 3,4,5-tris(hexadecyloxy)benzohydrazide (1 mmol) and p-toluenesulfonic acid (0.05 mmol, as a catalyst) were added to ethanol (15 mL) and chloroform (5 mL). Then the reaction mixture was stirred under refluxed conditions for 24 hours, after removing the solvent, yielding the precipitate of **G1**.(Yield, 25%). The solid of **G1** was getted by column chromatography. ^{1}H NMR ($CDCl_3$, 400 MHz): δ, 9.98 (s, 1H,-NH), 8. 46 (s, 1H, -N=CH), 8.26 (s, 1H, -ArH), 8.03-8.01 (d, 1H, J = 8.0 Hz, -ArH), 7.80-7.79 (d, J = 8.0 Hz, 1H, -ArH), 7.71 (s, 1H, -ArH), 7.55 (m, 1H, -ArH), 7.27-7.26 (d,J = 1.6 Hz,- ArH), 7.10(s, 2H, -ArH) 3.96 (s, 6H, $-OCH_2$), 1.78 (t, J = 6.9 Hz, 6H, $-OCH_2CH_2$), 1.43~1.26 (m, 72H, $-CH_2$), 0.86 (t, J = 6.2 Hz, 9H, $-CH_3$). ^{13}C-NMR ($CDCl_3$, 100 MHz) δ/ppm 164.40, 153.38, 148.09, 147.65, 136.47, 129.83, 128.35, 127.71, 118.35, 106.15, 77.21, 77.00, 76.79, 73.47, 69.17, 31.92, 30.36, 29.67, 29.43, 29.37, 29.33, 26.05, 22.68, 14.10. IR (KBr, cm^{-1}) v: 3432 (N-H), 1650 (C=O), 1585 (C=N); MS-ESI calcd for $C_{65}H_{109}N_3O_4$ $[G1 + H]^+$: 996.8400; found: 996.7500.

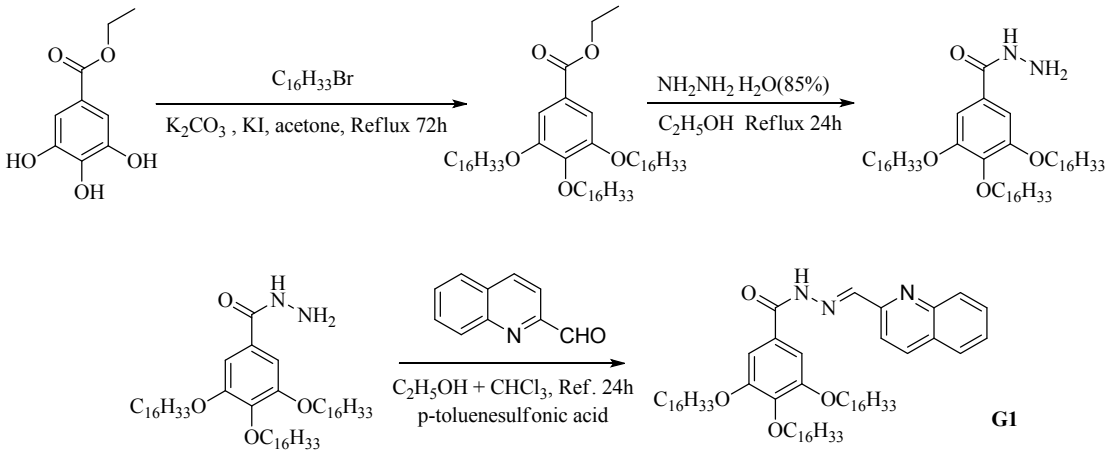

Scheme S1. Synthesis of the gelator **G1**.

Table S1 . Gelation Property of Organogelator **G1**

Entry	Solvent	State[a]	CGC[b]	Tgel[c] (℃, wt%)
1	Cyclohexane	S	\	\
2	Toluene	S	\	\
3	Petroleum ether	S	\	\
4	THF	S	\	\
5	Chloroform	S	\	\
6	Dichloromethae	S	\	\
7	Acetone	G	1.0	43(1.5%)
8	Acetonitrile	P	\	\
9	DMF	G	0.6	45(1.0%)
10	DMSO	P	\	\
11	Methanol	P	\	\
12	Ethanol	G	0.4	69(1.0%)

[a]G, P and S denote gelation, precipitation and solution, respectively, c = 0.8%.
[b]The critical gelation concentration (wt%, 10mg/mL = 1.0%).

[c]The gelation temperature(℃).

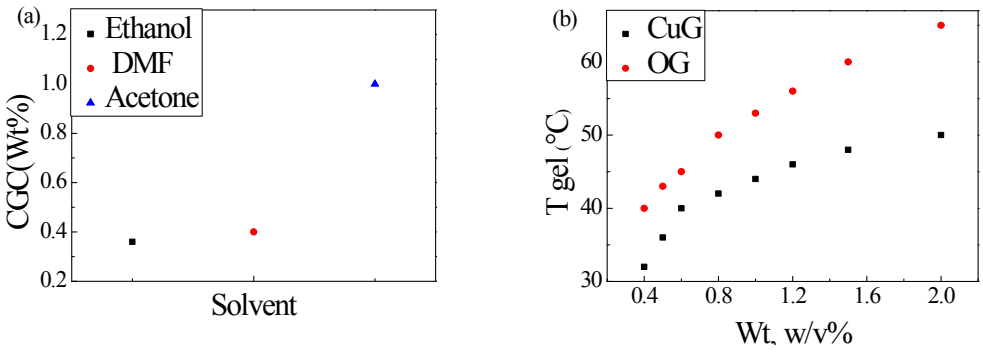

Figure S1. a) Plots of CGCs of **G1** in the different solvents. b) Plots of T_{gel} against the concentrations of organogel **OG** and metalogels **CuG** in DMF.

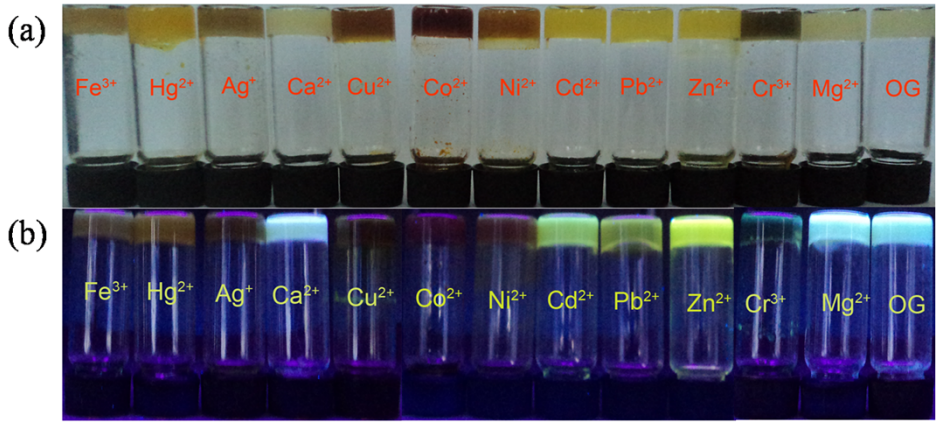

Figure S2. Photographs of organogel of **G1** in DMF (1% w/v) and organogels of **G1** in the presence of various metal ions (using their perchlorate salts as the sources, **G1**: cation =2 : 1) under (a) room (b) UV light.

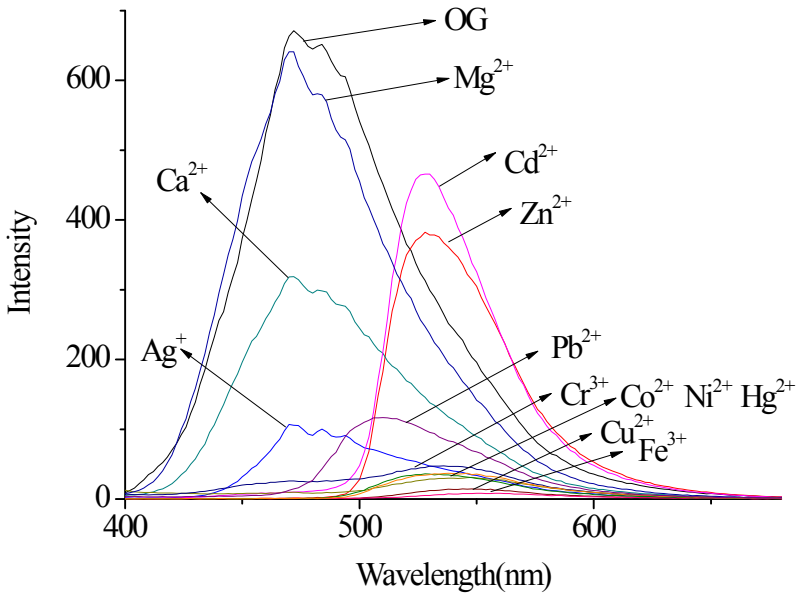

Figure S3. Fluorescence spectra of organogel of **G1** in DMF (0.8% w/v) and organogels of **G1** in the presence of various metal ions (using their perchloric salts as the sources) added in 2 : 1 mol ratio with respect to **G1** (λ_{ex} = 380 nm)**.**

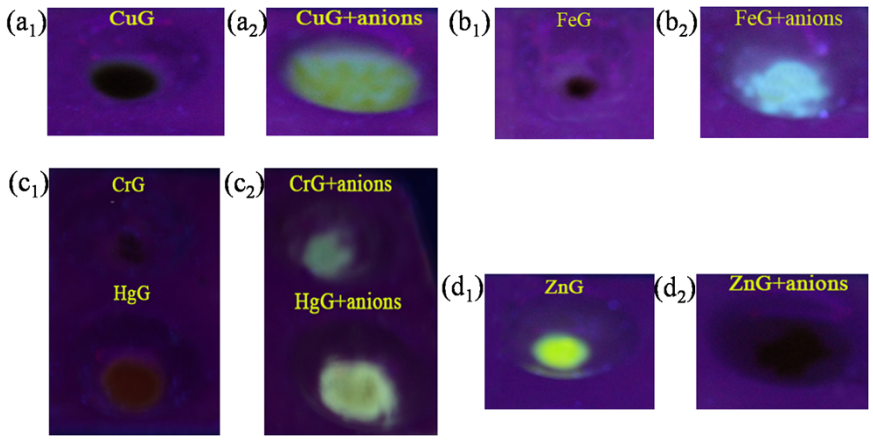

Figure S4. Fluorescence responses of the metallogels-based sensor to the presence of 1 equiv. of anions mixture (a water solution containing the mixture of F^-, Cl^-, Br^-, I^-, AcO^-, $H_2PO_4^-$, N_3^-, SCN^-, S^{2-}, ClO_4^- and CN^-). (a_1) **CuG**; (a_2) **CuG** and anions; (b_1) **FeG**; (b_2) **FeG** and anions; (c_1) **CrG** and **HgG**; (c_2) **CrG** and anions, **HgG** and anions; (d_1) **ZnG**; (d_2) **ZnG** and anions.

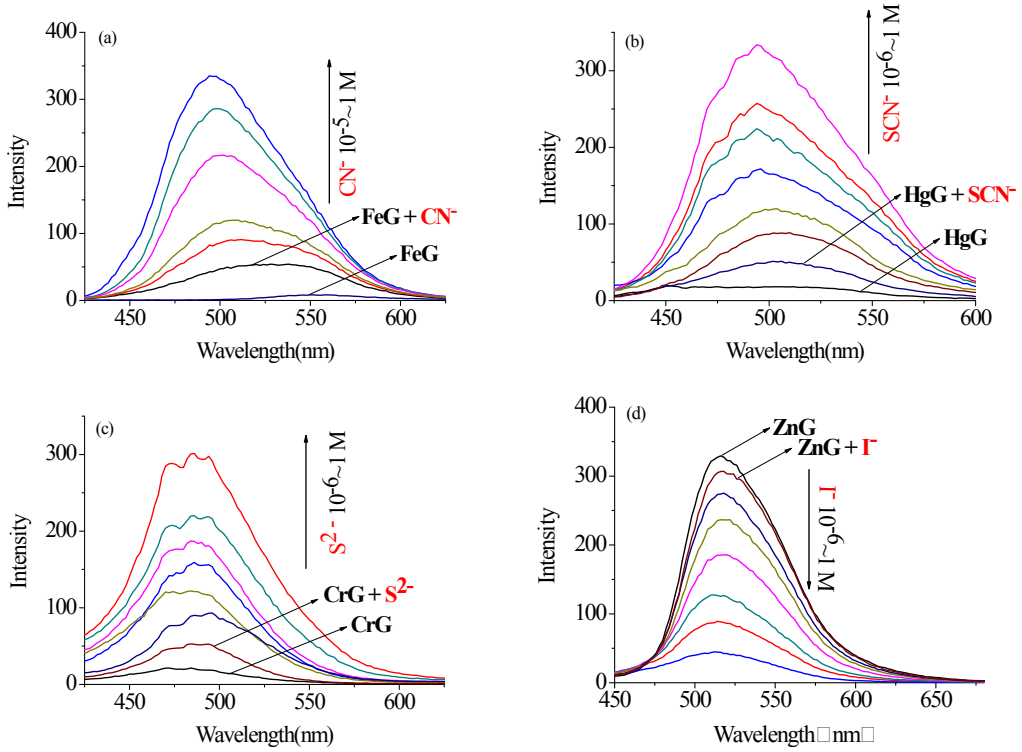

Figure S5. a) Fluorescence spectra of **FeG** (1.0%, in DMF) with increasing concentration of CN^- (using 1.0 mol L^{-1} NaCN water solution as the CN^- sources), λ_{ex} = 380 nm; b) Fluorescence spectra of **HgG** (1.0%, in DMF) with increasing concentration of SCN^- (using 0.1 mol L^{-1} KSCN water solution as the SCN^- sources), λ_{ex} = 380 nm; c) Fluorescence spectra of **CrG** (1.0%, in DMF) with increasing concentration of S^{2-} (using 0.01 mol L^{-1} Na_2S water solution as the S^{2-} sources), λ_{ex} = 380 nm; d) Fluorescence spectra of **ZnG** (1.0%, in DMF) with increasing concentration of I^- (using 0.1 mol L^{-1} KI water solution as the I^- sources), λ_{ex} = 380 nm.

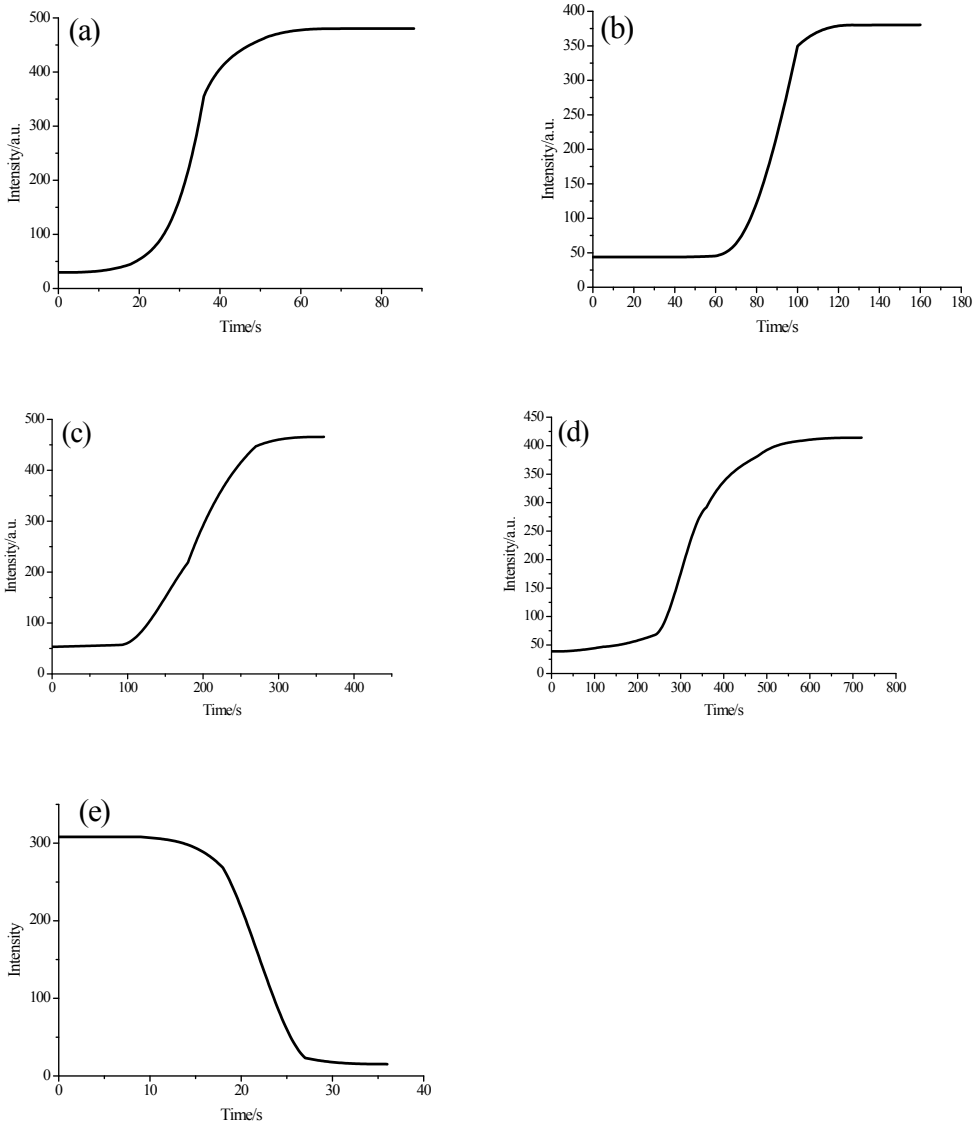

Figure S6. Time-dependency fluorescence spectra of a) **CuG** film treated with CN^-, 0.01 mol L^{-1} NaCN water solution as the CN^- sources, λ_{ex} = 380 nm; b) **FeG** film treated with CN^-, 0.01 mol L^{-1} NaCN water solution as the CN^- sources, λ_{ex} = 380 nm; c) **HgG** film treated with SCN^-, 0.01 mol L^{-1} KSCN water solution as the SCN^- sources, λ_{ex} = 380 nm; d) **CrG** film treated with S^{2-}, 0.01 mol L^{-1} Na_2S water solution as the S^{2-} sources, λ_{ex} = 380 nm; e) **ZnG** film treated with I^-, 0.01 mol L^{-1} KI water solution as the I^- sources, λ_{ex} = 380 nm

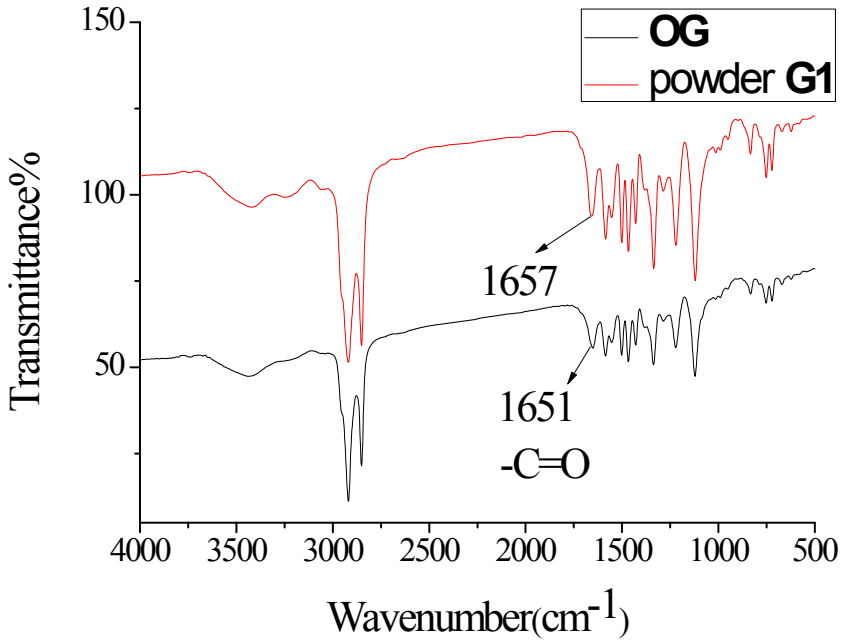

Figure S7. FT-IR spectra of powdered **G1** and xerogel of organogel **OG**.

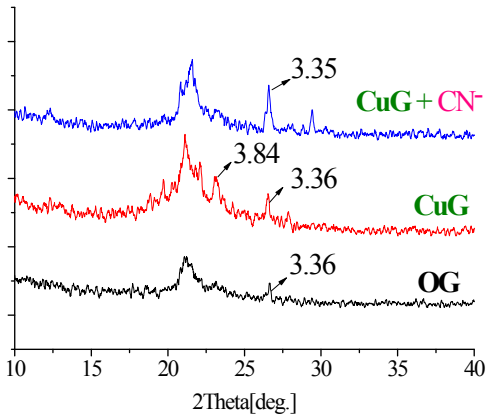

Figure S8. Powder XRD patterns of xerogel of **OG**, **CuG**, and **CuG** xerogel treated with CN^-.

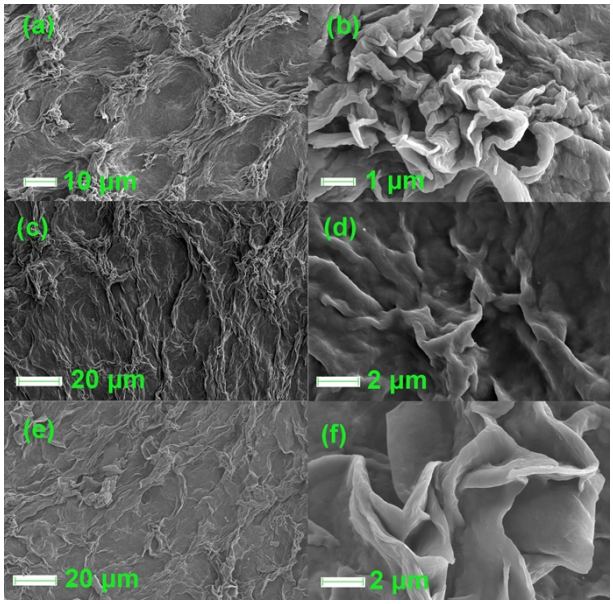

Figure S9. SEM images of (a) and (b) **OG** xerogel; (c) and (d) **CuG** xerogel and (e) and (f) **CuG** xerogel treated with CN- in situ.

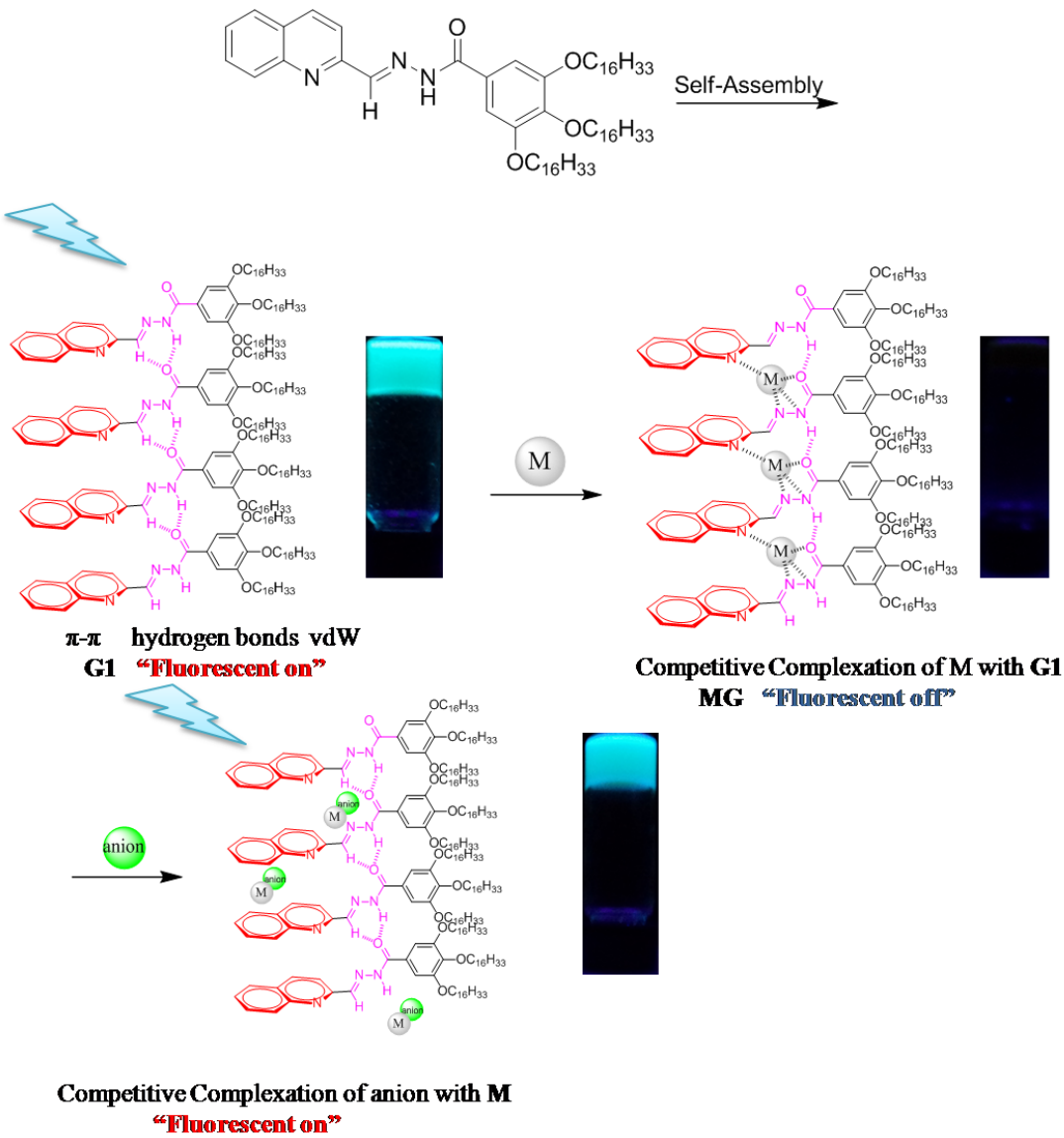

Scheme S2. Chemical structure of the **G1** and the assumed self-assembly and stimuli-responsive mechanism.